USING TIDALLY DRIVEN ELASTIC STRAINS TO INFER REGIONAL CRUSTAL THICKNESS AND OCEAN SALINITY AT ENCELADUS A. Berne[1], M. Simons[1] , J. Keane[2] , and R. Park[2], [1]California Institute of Technology, 1200 E California Blvd., Pasadena, CA 91125, USA; aberne@caltech.edu [2]NASA Jet Propulsion Laboratory, 4800 Oak Grove Dr, Pasadena, CA 91109, USA

Introduction: Saturn's small moon Enceladus is a geologically active and potentially habitable ocean world (Porco *et al*., 2006). Jets near the South Pole of Enceladus supply material from a global subsurface ocean (Thomas *et al*., 2016) to a water-ice plume. Cassini mass spectrometry found that crystals in the plume contain salt species including NaCl, $NaHCO_3$, Na_2CO_3, and KCl (Postberg *et al*., 2009). The abundance of detected salt species in the ocean of Enceladus mediates habitable conditions on the satellite (e.g., pH and temperature range). Moreover, the composition of plume samples may not be representative of that of the ocean due to species fractionation as material is ejected from jets. Independent determinations of ρ_w should directly constrain absolute abundances of salt species expected in Enceladus's ocean (Vance *et al*., 2021).

Geodetic measurements can be used to infer ρ_w. Static (i.e., unchanging at the diurnal timescale) gravitational potential external to Enceladus is sensitive to topography at density interfaces within the interior of the satellite. Joint measurements of static topography at the outer surface and static gravitational potential can therefore be used to infer ρ_w but require a-priori knowledge of outer ice shell density ρ_{ice} and the spatially variable thickness of the outer ice shell d. Spectroscopic measurements of scattered light from icy material at the outer surface permit robust inferences of ρ_{ice} (Vance *et al*., 2021). However, independent (i.e., of assumed ρ_w) methods to determine d across the crust do not currently exist for Enceladus.

Diurnal eccentricity tides cyclically deform Enceladus over the satellite's orbital period (i.e., 32.9 hrs). Elastic deformation within the crust in response to tidal forces is sensitive to d at both global and regional spatial scales (Berne *et al*., 2022). At the global scale, the integrated effect of lateral variations in crustal thickness biases inferences of bulk structure (e.g., mean effective elastic thickness) from measurements of long-wavelength surface displacement (Berne *et al*., 2022). However, at regional scales strain rate is sensitive to the local cross-sectional area of the crust which accommodates tidally-induced stress fields. Lateral variations in d therefore imply spatial variations in measurable elastic strain rate (e.g., the second invariant of the horizontal deviatoric elastic strain rate averaged over the tidal cycle: ξ).

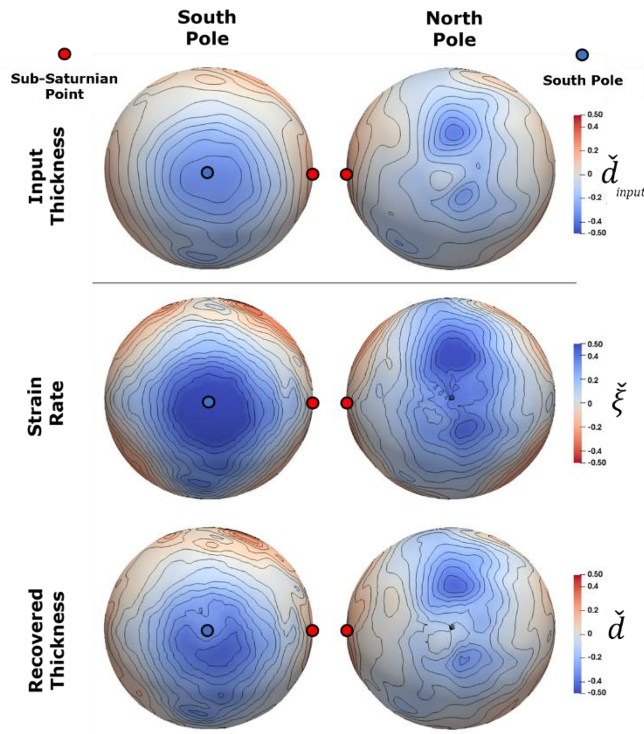

Figure 1*: Snapshots of model input crustal thickness $\check{d}_{input}$ (top row), the simulated 2nd invariant of horizontal deviatoric strain rate $\check{\xi}$ averaged over the 32.9 hr tidal cycle (center row), and recovered crustal thickness $\check{d}$ (bottom row) (see Equation 1) viewed facing south and north poles at Enceladus. The horizontal line denotes a separation between model inputs (above) and outputs (below). Plotted contours denote colorscale intervals of 0.05. Sub-Saturnian point and South Pole locations are labelled.*

Results: In this work, we explore the challenge of inferring the spatially variable thickness of outer ice of Enceladus using measurable elastic deformation. We simulate strain rates on tidally-loaded quasi-spherical shells using numerical finite element models (FEMs) which can incorporate lateral variations in crustal thickness. We perform simulated recoveries of d from models and quantify mismatch between input thickness fields d_{input} and recovered thickness fields d. We conclude by highlighting the feasibility of combining our analysis with measurements of static topography and gravitational potential to infer ρ_w at Enceladus.

We define the non-dimensional parameters $\check{\xi}$, $\check{d}$, $\check{d}_{input}$, and τ relevant for our investigation (d_0 denotes mean elastic thickness of models with variations in crustal thickness; ξ_0 denotes strain evaluated on a spherically symmetric model with uniform thickness d_0). Note that τ describes the coherence between input and recovered crustal thicknesses from our analysis:

$$\check{\xi} = \log(\xi/\xi_0) \quad (1a)$$

$$\check{d} = \log(d/d_0) \quad (1b)$$

$$\check{d}_{input} = \log(d_{input}/d_0) \quad (1c)$$

$$\tau = \left(1 - \left|\frac{d - d_{input}}{d_{input}}\right|\right) * 100 \quad (1d)$$

We find a broad spatial correlation between effective local stiffness and strain rate enabling computations of $\check{d}$ (see Figure 1 and Equation 1b). Computed $\check{\xi}$ (see Equation 1a) fields reflect regional thinning at north and south poles, crustal thickening at low latitudes, and the significant asymmetry in crustal thinning between northern and southern hemispheres visible in $\check{d}_{input}$ (see Equation 1c). We find that our analysis most correctly predicts d at very long spatial wavelengths (i.e., spherical harmonic degrees $l < 10$) (see Figure 2). Propagating uncertainty for conditions expected at Enceladus, we find that computed error in the of variation of d at long spatial wavelengths yields a range of inferred ρ_w of about 3 kg/m^3 (i.e., a range of ocean salinities spanning 3 g/l). For comparison, determinations of ρ_w and ocean salinity from mass spectrometry yield ranges of 50 kg/m^3 and 50 g/l respectively. Inferences of salinity at the 5 g/l precision level (i.e., as opposed to the 50 g/l precision level) would dramatically constrain the expected pH and temperature range in Enceladus's ocean (Vance *et al.*, 2021).

Interferometric Synthetic Apreture Radar (InSAR) measurements from orbiting platforms readily enable the analysis described in this work. Maximum peak-to-peak (i.e., over the tidal cycle) horizontal and radial displacements associated with the presence of crustal thickness variations at Enceladus (i.e., relative to spherically symmetric models) are approximately ± 1-10 cm (Berne *et al.*, 2022). These values are substantially larger than the demonstrated sensitivity of InSAR measurements to ground displacement (e.g., Simons & Rosen, 2015). We therefore envision a mission equipped with InSAR could feasibly assess habitable conditions and characterize detailed regional structure of the crust of Enceladus.

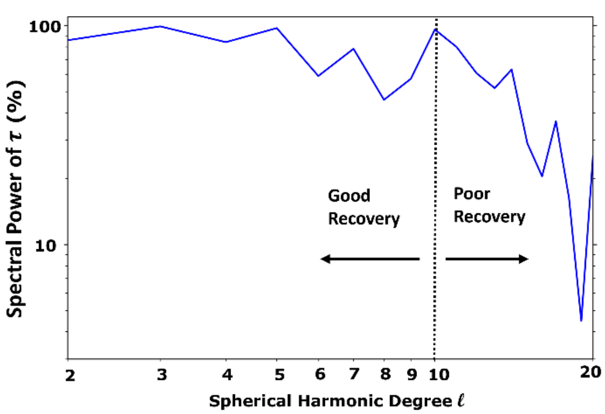

Acknowledgments: This research was supported by the Future Investigators in NASA Earth and Space Science and Technology (FINESST) Program and a Strategic Research and Technology Development at the Jet Propulsion Laboratory, California Institute of Technology, under a contract with NASA.

References:

Berne, Alexander, et al. "Inferring the Mean Effective Elastic Thickness of the Outer Ice Shell of Enceladus from Diurnal Crustal Deformation." Authorea Preprints (2022).

Porco, Carolyn C., et al. "Cassini observes the active south pole of Enceladus." science 311.5766 (2006): 1393-1401.

Postberg, Frank, et al. "Sodium salts in E-ring ice grains from an ocean below the surface of Enceladus." Nature 459.7250 (2009): 1098-1101.

Simons, M., and P. A. Rosen. "Interferometric synthetic aperture radar geodesy." Geodesy 3 (2007): 391-446.

Thomas, P. C., et al. "Enceladus's measured physical libration requires a global subsurface ocean." Icarus 264 (2016): 37-47.

Vance, Steven, et al. "Distributed geophysical exploration of Enceladus and other Ocean Worlds." Bull. Am. Astron. Soc. 4 (2021).

Figure 2*: Scale dependance of recovered vs. input thickness coherence. Plot shows the spectral power of the spherical harmonic expansion of* τ *(see Equation 1d). 100% indicates a perfect recovery of crustal thickness from FEMs. Dotted line denotes cutoff at spherical harmonic degree* $l = 10$ *between good and poor recoveries of crustal thickness from elastic strains.*